LAWRENCE LIVERMORE NATIONAL LABORATORY

LLNL-CONF-557603

The NIF 4.5-m nTOF Detectors

M. J. Moran, E. J. Bond, T. J. Clancy, M. J. Eckart, H. Y. Khater, V. Yu. Glebov

May 15, 2012

19th Topical Conference, High-Temperature Plasma Diagnostics
Monterey, CA, United States
May 6, 2012 through May 10, 2012

Disclaimer

The NIF 4.5-m nTOF Detectors

M.J. Moran[1], E.J. Bond[1], T.J. Clancy[1], M.J. Eckart[1], H.Y. Khater[1], V.Yu. Glebov[2]

[1]*Lawrence Livermore National Laboratory, Livermore, CA, 94551*
moran3@llnl.gov

Laboratory for Laser Energetics, University of Rochester, Rochester, NY 14623-1299, vgle@lle.rochester.edu

The first several campaigns of laser fusion experiments at the National Ignition Facility (NIF) included a family of high-sensitivity scintillator/photodetector neutron-time-of-flight (nTOF) detectors for measuring DD and DT neutron yields. The detectors provided consistent neutron yield benchmarks from below 1E9 (DD) to nearly 1E15 (DT). The detectors demonstrated DT yield measurement precisions better than 5%, but the absolute accuracy relies on cross calibration with independent measurements of absolute neutron yield. The 4.5-m nTOF data have provided a useful testbed for testing improvements in nTOF data processing, especially with respect to improving the accuracies of the detector impulse response functions. The resulting improvements in data analysis methods have produced more accurate results. In summary, results from the NIF 4.5-m nTOF detectors have provided consistent measurements of DD and DT neutron yields from laser-fusion implosions.

I. INTRODUCTION

Laser-driven Inertial Confinement Fusion (ICF) experiments at the National Ignition Facility (NIF) require accurate measurement of yield, ion temperature (T_{ion}), and downscattered neutron fraction (dsf) on DD andDT fusion experiments. Previous publications describe a staged sequence of neutron time-of-flight (ntof) detectors that perform these measurements, providing reliable consistent results over a neutron yield range from below 10^9 to nearly 10^{15}.[1] The basic detector design consists of a photodetector (a photodiode or photomultiplier) butt-coupled to a 40-mm diameter BC-422(or BC-422Q1%) scintillator, housed in a 2.5-cm thick lead pig, and placed inside an atmospheric-pressure diagnostic well that extends from the target chamber port (at ≈ 5.5 m) to within 4.5m of the target position. The choice of scintillator and photodetector gain (approximately 1, 10^3, or 10^6) provides the necessary staging of sensitivity as NIF experiments progress to higher and higher neutron yields. Remotely installed Tektronix 7104 digitizers record electrical signals from the detectors.

A typical example of data is fast single pulse whose integral is proportional to the neutron yield, whose width increases with the ion temperature of the burning plasma, and whose late tail indicates the fraction of neutrons that scatter to lower energies as they propagate out of the target (the dsf). The traditional data analysis method finds the Gaussian pulse which, when convolved with a simple response function, provides an optimal match to the recorded signal.[2] This so-called “forward-fit” method benefits from the strength of the underlying statistics of ntof signals, while avoiding the signal distortion issues that accompany Fourier deconvolution. The integral of the Gaussian pulse provides the inferred neutron yield and the FWHM of the Gaussian provides the ion temperature measurement. This method provides accurate results for DD and DT neutron yields, and consistent results for the inferred T_{ion}.

II. METHOD

The forward-fit method compares the measured data with the convolution of a test Gaussian neutron spectrum with the detector impulse response function (IRF). The optimized match between data and convolution then identifies the experimental Gaussian neutron spectrum for that measurement. The traditional IRF is the convolution of an exponential decay with a (detector) Gaussian.[2] This Gaussian contribution represents the relatively fast impulse response of the photodetector ($\leq$ 1 ns) alone, while the exponential decay represents the slower ($\geq$ 1 ns) contributions from scintillator decay and prompt backgrounds from scattered neutrons. This method provides a reasonable description for this detector design, and there is a long history of consistent and accurate results from ntof data analysis that relies on this kind of IRF.

The desire to improve accuracy and to extract additional information from ntof data has motivated the development of IRFs that are based on recorded data for each detector. The additional information that can be recovered includes improved precision of Tion, neutron bangtime, the downscattered neutron fraction (dsf), and the full neutron spectrum. The individual IRFs can be constructed with several different methods, depending on the information that is available for each detector. In some cases laboratory calibration of individual components can be convolved with Monte Carlo simulations of scattered neutron signals to produce an overall IRF.

With the 4.5-meter nTOFDTLO (a BC-422Q scintillator with single-stage microchannelplate photomultiplier), measurements of cosmic ray impulses provided a direct measurement of the overall system response. The system response was convolved with Monte-Carlo simulations of scattered neutron signals to produce the overall IRF. The 4.5-meter nTOFDTHI (BC-422Q scintillator with a photodiode) has no net gain, so that cosmic rays do not produce measurable signals. The DTHI IRF is obtained by deconvolving a Gaussian neutron signal from the recorded signal of an “exploding pusher” experiment (which is believed to produce a Gaussian neutron pulse with a single well defined T_{ion}).

The advantages of deconvolving a Gaussian from an exploding pusher include inferring the overall system IRF in situ and establishing accurately the late tail of the neutron IRF. The disadvantages include errors from an incorrect Gaussian temperature or non-Gaussian contributions to the neutron spectrum 14-MeV peak.

III. EXPERIMENT

The IRF for the NIF ntofDTHI detector was obtained by deconvolving a Gaussian pulse from the signal recorded on an exploding pusher shot on November 21, 2011. Figure 1 shows the DTHI recorded signal, the “fit” to the signal, and the IRF that from the deconvolution of a 5.7-keV Gaussian pulser from the data. The 5.7-keV Gaussian temperature is provided by more accurate ntof detectors that are located approximately 22m from the target. The deconvolution is accomplished by a “Richardson-Lucy” maximum likelihood iterative reconstruction method.[3] A re-convolution of the resulting IRF with the 5.7-keV Gaussian produces the “fit” shown in Figure 1, demonstrating that the IRF is consistent with the recorded data. The IRF was tested further by deconvolving it from the recorded data to verify that it does reproduce the original Gaussian accurately.

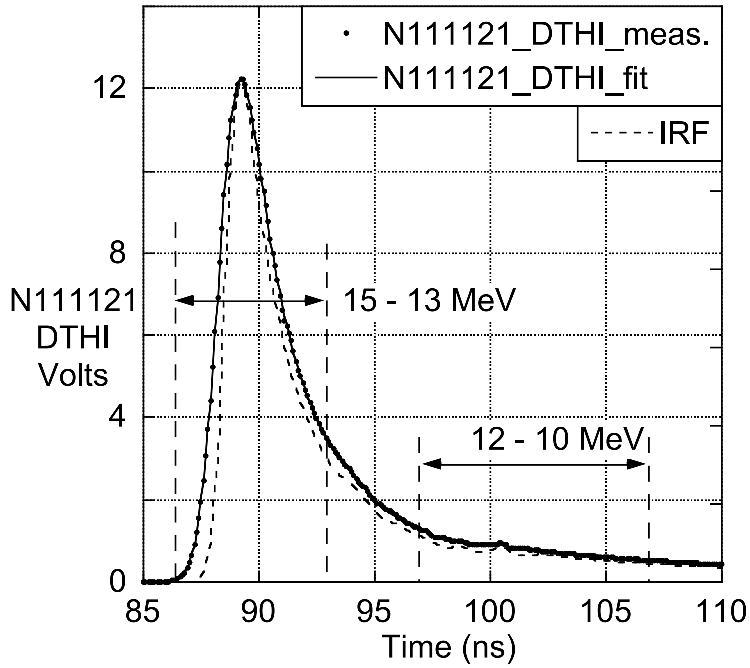

Figure 1 Comparison of data to fit with IRF

The self-consistency checks of the IRF are necessary because there is no method for identifying the perfect IRF, and all ntof IRFs are known to have finite errors. For example, when the DTHI IRF is used in a “forward fit” to the exploding pusher signal, the resulting T_{ion} is 5.34 keV = 360 eV less than the original 5.7-keV Gaussian. However, for this IRF (with FWHM ≈ 2.5 ns), 360 eV corresponds to an error in the width of approximately 20 psec. The ntof data is recorded in 100-psec time bins, so that an estimated error of 20 psec represents the achievement of very high precision from the data.

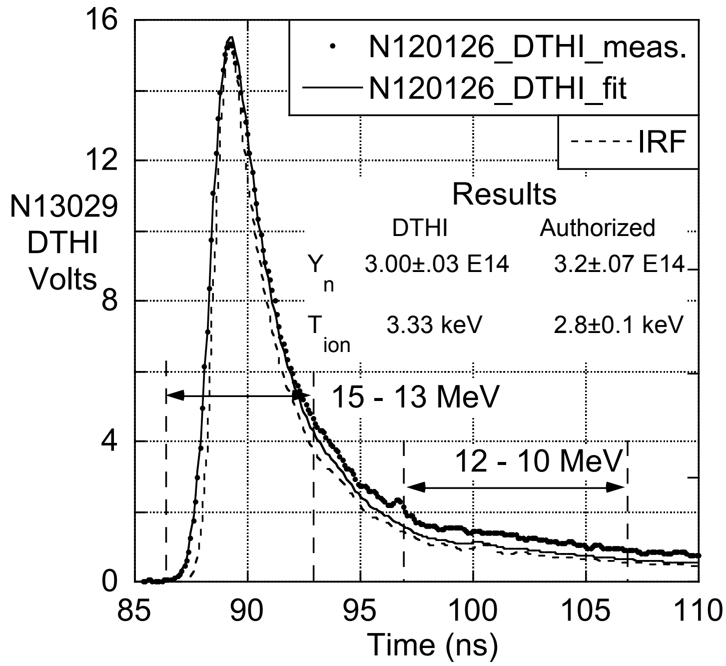

Figure 2 Comparison of forward fit with data on DT experiment N120126

Figure 2 shows the DTHI data and analysis for a DT layered target experiment with a yield of $1.4*10^{13}$ neutrons. The plot shows the recorded data, the fit to the data, and the IRF (from Fig 1) that was used to construct the fit. Here, the general agreement between the recorded data and the fit are not as good as in Fig. 1, especially on the tail of the pulse. In fact, the fit is constrained to optimize agreement with the data over the leading edge and halfway down the tail of the pulse. The later discrepancy between the data and the fit is direct evidence of downscattered neutron fluxes that are not present with the exploding pusher targets (Fig 1). Although the presence of the downscattered neutron contributions is clear, this data does not provide a simple result for the downscattered neutron fraction. The dsf is the ratio of neutrons with energies from 10-12 MeV to those with 13-15 MeV. Because of the relatively broad IRF of DTHI, those energy regions (indicated by dotted lines) are not accurately delineated in the raw DTHI data.

The most important purpose of the DTHI data is to provide a consistent prompt result for DT neutron yield in NIF experiments. Credible yield measurement rely on using an accurate detector IRF and establishing an accurate absolute calibration for the detector sensitivity. Figure 1 describes the source of the DTHI IRF. The absolute calibration of sensitivity has been established by comparison of the integrated DTHI signal with first-principle absolute measurements of DT yield on a series of DT exploding pusher experiments. Zirconium activation, copper activation, and proton-recoil (MRS) diagnostics are combined to establish the authorized yields for the calibration.

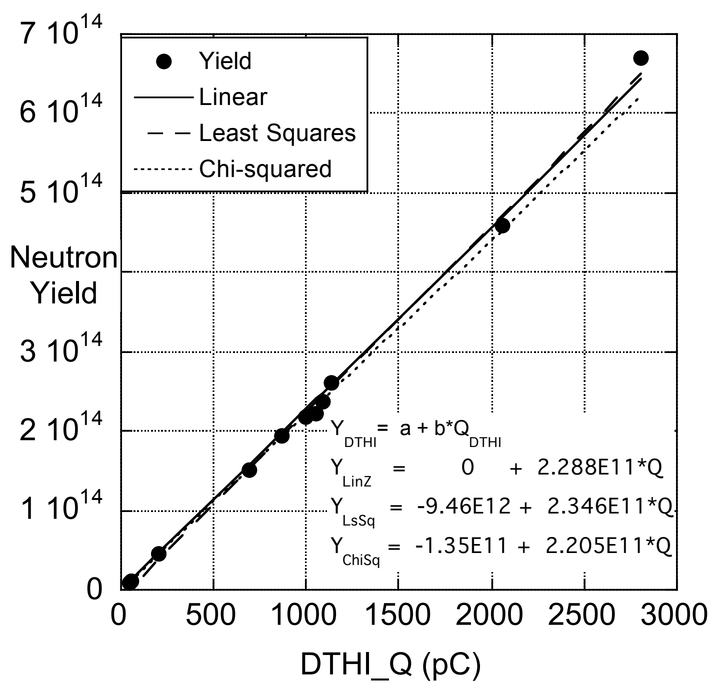

Figure 3 Fit of DTHI yield results to DT exploding pusher experiments

Figure 3 shows a comparison of the DTHI charge integral with the authorized yields. The signal charge has a clear linear relationship with the authorized yields, but the precise value of the linear calibration constants depend on the method used to fit the data to the yield. The plot displays the fits that result from three different methods: least squares fit with zero intercept, an unconstrained intercept least squares fit, and a chi-squared fit that weights the importance of each data point inversely to the precision of that result. The zero intercept least squares fit is the value that was used until January, 2012. However, the calibration now has been updated by the chi-squared fit. The new fit results in a 4%-reduction in linear sensitivity, but provides a result for the DTHI calibration precision of 1%. The overall accuracy of the DTHI yields will scale with the accuracy of the benchmark yields, about 7%.

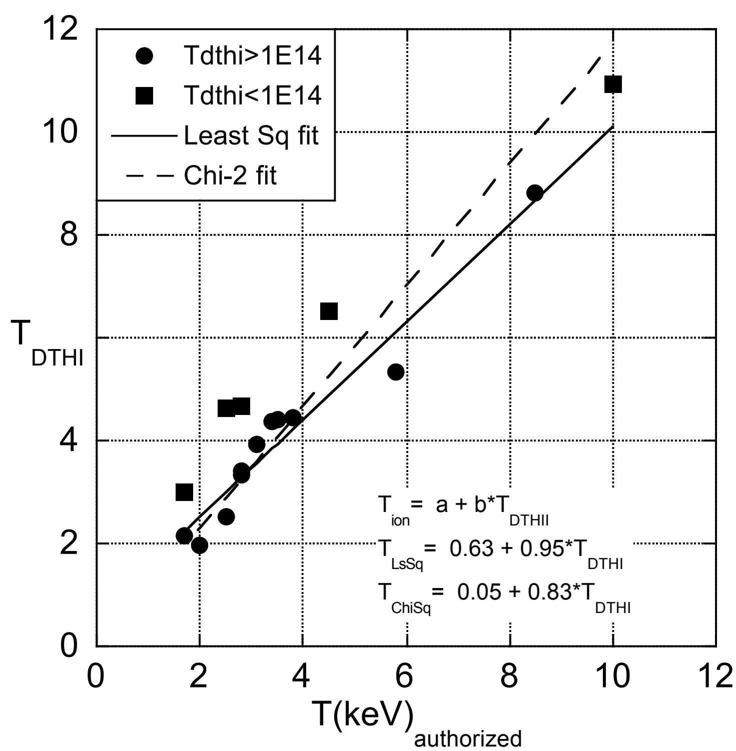

Figure 4 Fit of DTHI T_{ion} results for DT exploding pusher experiments

The DTHI data generally cannot be used to recover accurate measurements of ion temperature. The Tion of a DT nuclear burn results in a corresponding Gaussian broadening of the 14-MeV neutron peak.[4] The DTHI temperatures are unreliable because the FWHM of the IRF usually is a large fraction, compared to the Gaussian broadening. Even small errors in the shape of the IRF lead to large errors in the narrower inferred neutron pulse. For DTHI with a 3.5-keV ion temperature a 50 psec error in the IRF FWHM leads to an error of 0.75 keV in the inferred temperature. The relationship between the DTHI-inferred T_{ion}s and the authorized T_{ion}s can be studied in the same way that the neutron sensitivity calibration is established. Figure 4 shows a plot of the DTHI-inferred temperatures against the authorized values. The plot also shows least-square and chi-squared fits for the DTHI results. The fits do not include experiments with yields less than $1*10^{14}$, as these results show larger and unexplained errors. The least squares fit shows very good agreement with the authorized values, while the chi-squared fit shows a less optimistic fit that results from emphasizing data from experiments with the most accurate results.

IV. CONCLUSION

The 4.5-meter nTOF detectors have provided consistent measurements of neutron yield for all neutron-producing NIF experiments to date. Improvements in data processing methods have resulted in more accurate results and helped to extend the use of nTOF data to measurements of nuclear burn ion temperature and downscattered neutron measurements. This work performed under the auspices of the U.S. Department of Energy by Lawrence Livermore National Laboratory under Contract DE-AC52-07NA27344.

REFERENCES

[1]Glebov, V.Y., Rev. Sci. Instrum. 81, 10D325 (2010)

[2]Murphy, T.J., RSI, vol. 86, p. 610 (1997)

[3]Fister, T, Phys. Rev. B, 75, 174106 (2007)

[4]Brysk, H., Plasma Physics, Vol. 15, p. 611 (1973)

FIGURE CAPTIONS

Figure 1 Comparison of data to fit with IRF

Figure 2 Comparison of forward fit with data on DT experiment N120126

Figure 3 Fit of DTHI yield results to DT exploding pusher experiments

Figure 4 Fit of DTHI T_{ion} results for DT exploding pusher experiments

FIGURES

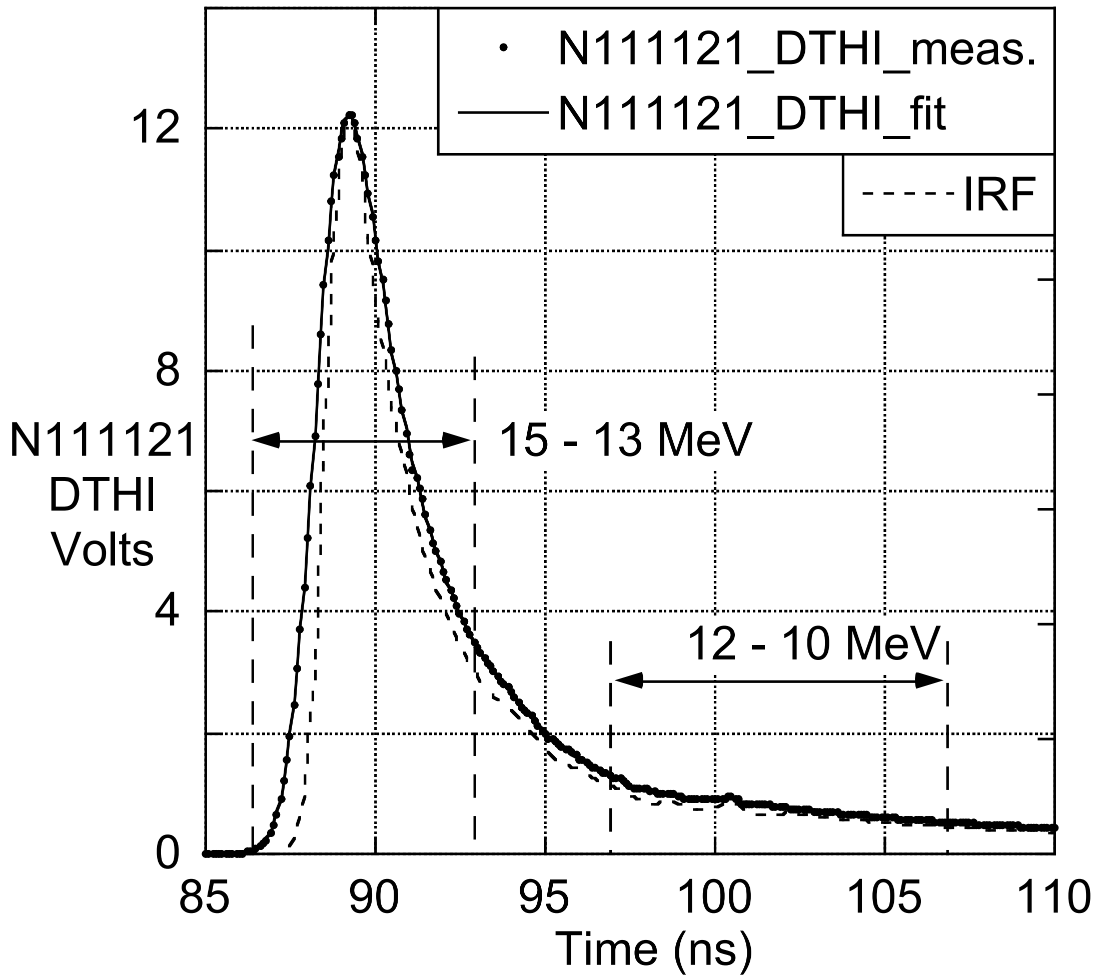
N111121_DTHI_meas.
N111121_DTHI_fit
IRF
15 - 13 MeV
12 - 10 MeV
N111121
DTHI
Volts
0
4
8
12
85
90
95
100
105
110
Time (ns)

Figure 1

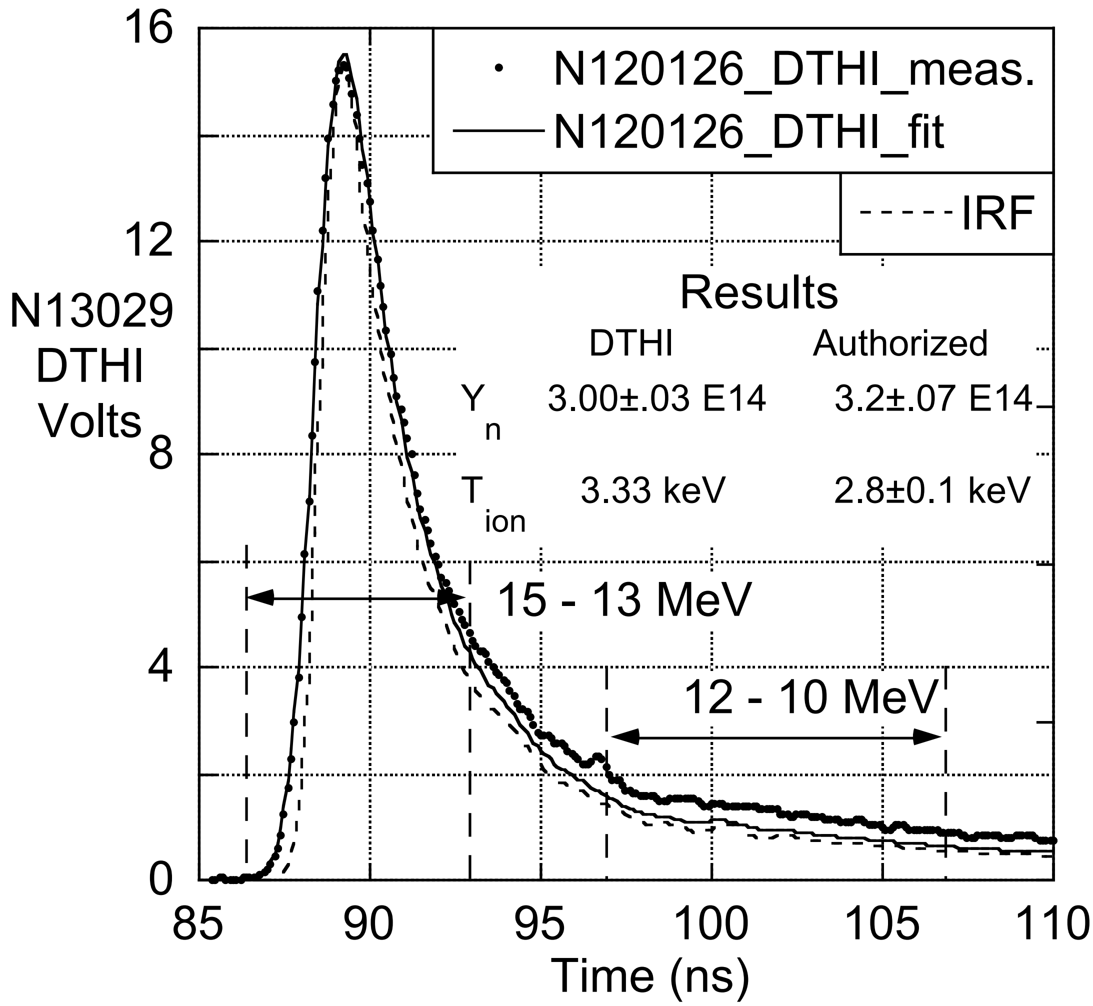
N120126_DTHI_meas.
N120126_DTHI_fit
IRF
Results
DTHI
Authorized
Y n 3.00±.03 E14 3.2±.07 E14
T ion 3.33 keV 2.8±0.1 keV
15 - 13 MeV
12 - 10 MeV
N13029 DTHI Volts
Time (ns)
0
4
8
12
16
85
90
95
100
105
110

Figure 2

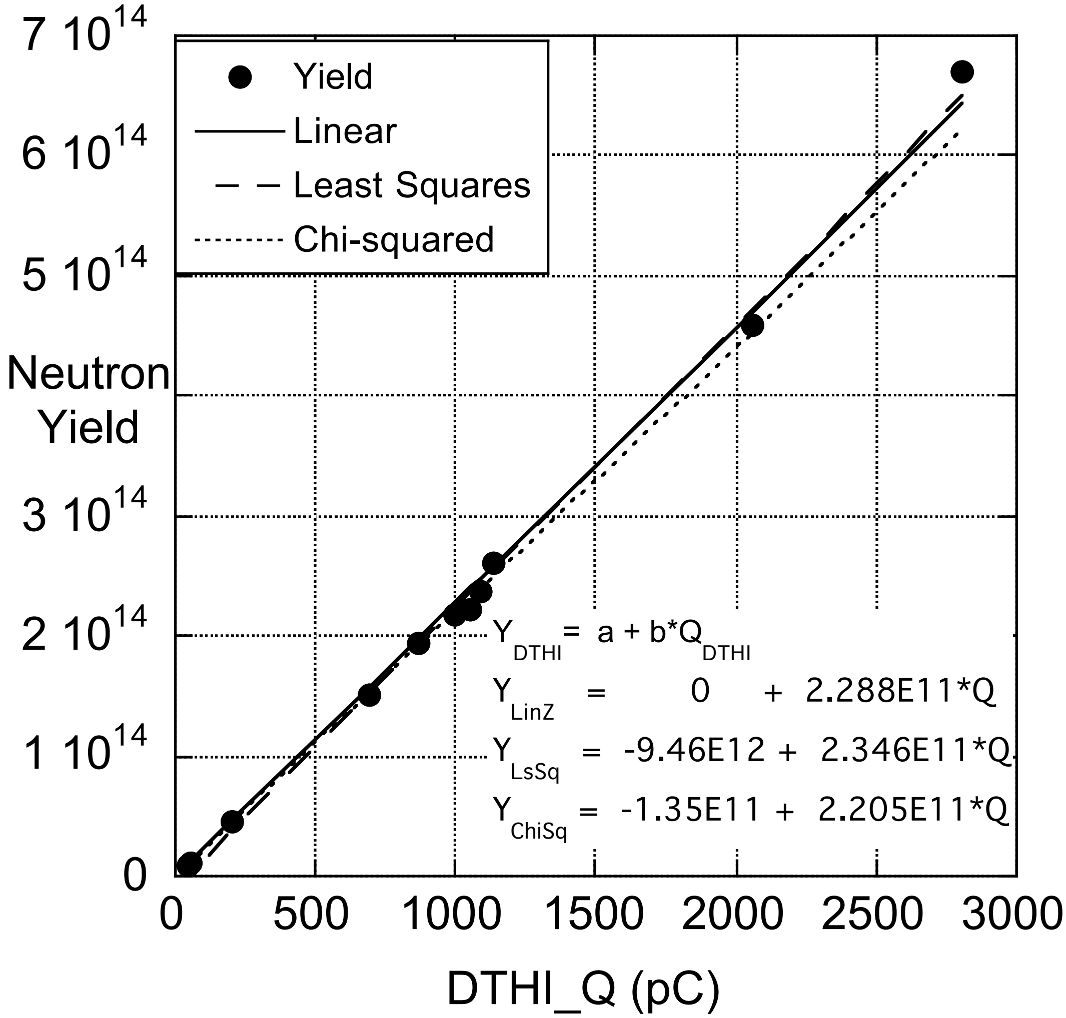

7 10^14
6 10^14
5 10^14
3 10^14
2 10^14
1 10^14
0
Neutron Yield
Yield
Linear
Least Squares
Chi-squared
$Y_{DTHI} = a + b*Q_{DTHI}$
$Y_{LinZ} = 0 + 2.288E11*Q$
$Y_{LsSq} = -9.46E12 + 2.346E11*Q$
$Y_{ChiSq} = -1.35E11 + 2.205E11*Q$
0
500
1000
1500
2000
2500
3000
DTHI_Q (pC)

Figure 3

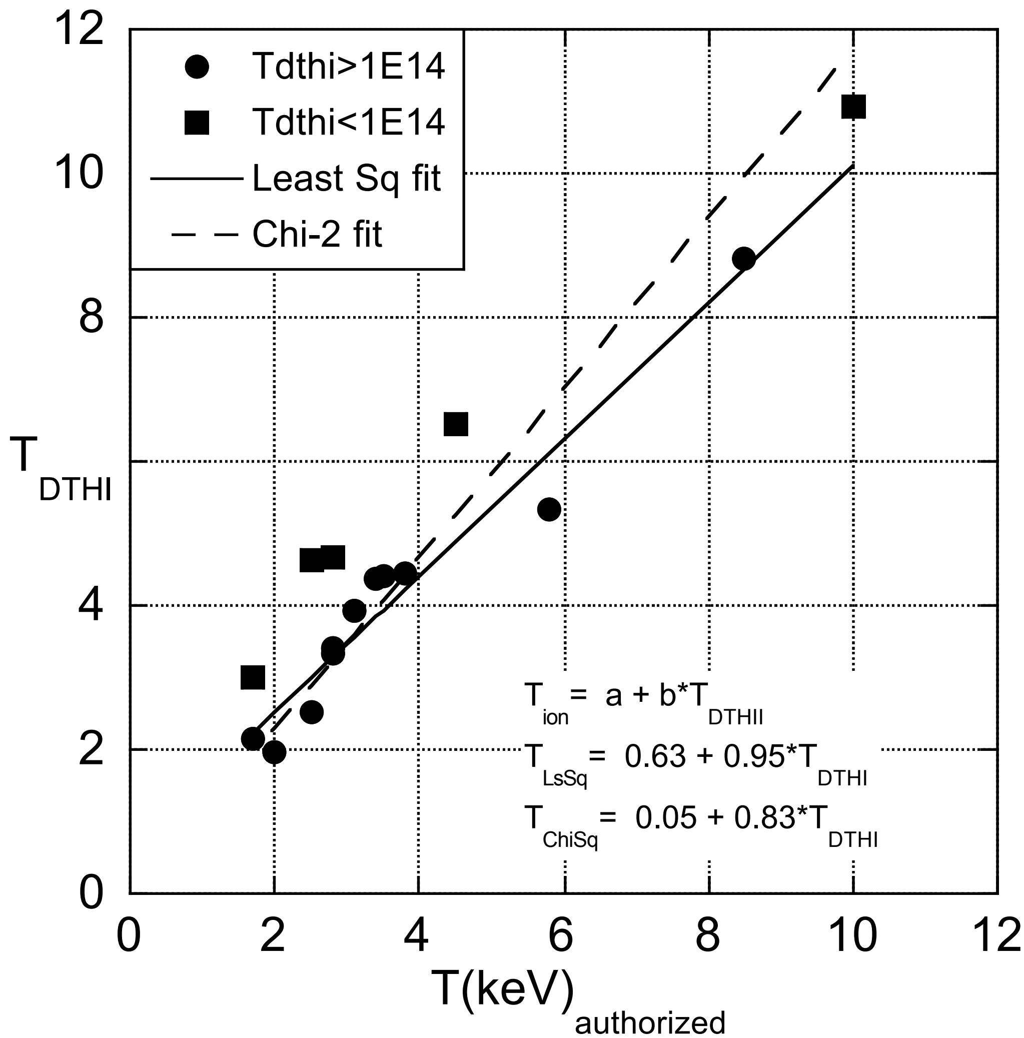

Tdthi>1E14
Tdthi<1E14
Least Sq fit
Chi-2 fit
T_ion = a + b*T_DTHII
T_LsSq = 0.63 + 0.95*T_DTHI
T_ChiSq = 0.05 + 0.83*T_DTHI
T_DTHI
T(keV)_authorized
0
2
4
6
8
10
12

Figure 4